Results in Physics 12 (2019) 2038–2043

Contents lists available at ScienceDirect

Results in Physics

journal homepage: www.elsevier.com/locate/rinp

The electronic and optical properties of MgO mono-layer: Based on GGA-mBJ

Bromand Nourozi[a,*], Amin Aminian[b], Narges Fili[c], Yousof Zangeneh[c], Arash Boochani[c], Pezhman Darabi[d]

[a] Young Researchers and Elite Club, Kermanshah Branch, Islamic Azad University, Kermanshah, Iran
[b] Department of Physics, University of Guilan, Rasht, Iran
[c] Department of Physics, Kermanshah Branch, Islamic Azad University, Kermanshah, Iran
[d] Department of Physics, Faculty of Science, University of Isfahan, HezarJerib Avenue, Isfahan 81746-73441, Iran

ARTICLE INFO

Keywords:
MgO mono-layer
GGA
mBJ
Optical properties
Electronic properties

ABSTRACT

The electronic and optical properties of MgO mono-layer were calculated based on the density functional theory (DFT) with FP-LAPW method using PBE-GGA and GGA-mBJ approximations. The electronic calculations of MgO mono-layer show a more interesting behavior than its bulk phase such as decreasing the band gap from 7.8 eV to 3.1 eV (for GGA) and 4.2 eV (for GGA-mBJ). Also, the MgO mono-layer has a direct band gap at Γ point in the Brillion Zone, and the effective masses of electrons are very greater than the effective mass of holes in this point. The optical coefficients such as dielectric parameters, energy loss functions, Refractions, Extinction and Absorption of this graphene-like (G-L) were calculated by RPA method which indicates the semiconducting properties of this mono-layer at the in-plane and perpendicular directions to emitting light.

Introduction

MgO compound has become one of the most interesting oxides in recent years for theoretical and experimental works. The MgO bulk might be crystallized in β1, β3 and β4 phases, and many attempts have been made to study the structure of thin films and cross section of MgO film on metal substrates [1–5]. The β1 phase has a rocksalt structure with the spatial group pf Fm3m(2 2 5). The β3 and β3 phases are crystallized in zinc blende and wurtzite structures respectively. Under normal conditions, MgO crystallizes in the rocksalt (B1) structure. This structure has been found to be stable at least up to 227 GPa [6]. Under pressure, the NaCl (B1) structure transforms into the CsCl (B2) structure. The transition pressure the inverted NiAs (B81) structure has an energy very similar to that of the CsCl structure [7]. The bulk structure of this matter has the possibility of construction and graphene structure growth due to its F.C.C geometric structure, by cutting along [1 1 1] direction. In the past years, it has been found that transitions from bulk to film and graphene phases cause basic and fundamental changes in the electronic, optical and even mechanical behavior of matters; here the prominent famous example is the behavior of Carbon Graphite turning to graphene structure as well as some other G-L compounds like Co_2VAl, MoS_2, Cu_2Si etc. [8–15], which their honeycomb structure and the special geometry governing the graphene structures and also existence of dangling bonds on the graphene surface leads to significant changes in the behavior of the compounds. The MgO bulk structure has the NaCl form with a band gap of experimental data about 7.77 eV [16], which implies its insulator-like behavior, however in all other computational reports using different codes, the band gap of this compound is found to be about 5–7.6 eV [17–24]. In recent years, the thin layer of MgO and its interface on metallic substrate has been considered more vastly, because of water interaction with this thin film [25–27]. Recent works have shown that the potential energy surface is extremely complex, and involves the interplay between several competing interactions: adsorbate–adsorbate, hydrogen-bonding, substrate–adsorbate, and in addition, partial dissociation of water molecules [28]. Mostly semiconductors have the energy gap in the 1 eV to 1.5 eV range and some others have the wide band gap around the 2 eV to 4 eV which their electronic and optical behaviors are fall in between the semiconductors and insulators. These semiconductors are used at much higher voltages, frequencies and temperatures, LEDs, lasers and radio frequency applications [29].

The novel aspect of our work is based on the fact that MgO-(G-L) structure formed of two nonplanar layers has not been investigated in optical properties and electronic transport aspects so far.

* Corresponding author.
E-mail address: bromanddalaho@yahoo.com (B. Nourozi).

https://doi.org/10.1016/j.rinp.2019.02.054
Received 28 October 2018; Received in revised form 20 January 2019; Accepted 16 February 2019
Available online 19 February 2019
2211-3797/ © 2019 Published by Elsevier B.V. This is an open access article under the CC BY-NC-ND license (http://creativecommons.org/licenses/BY-NC-ND/4.0/).

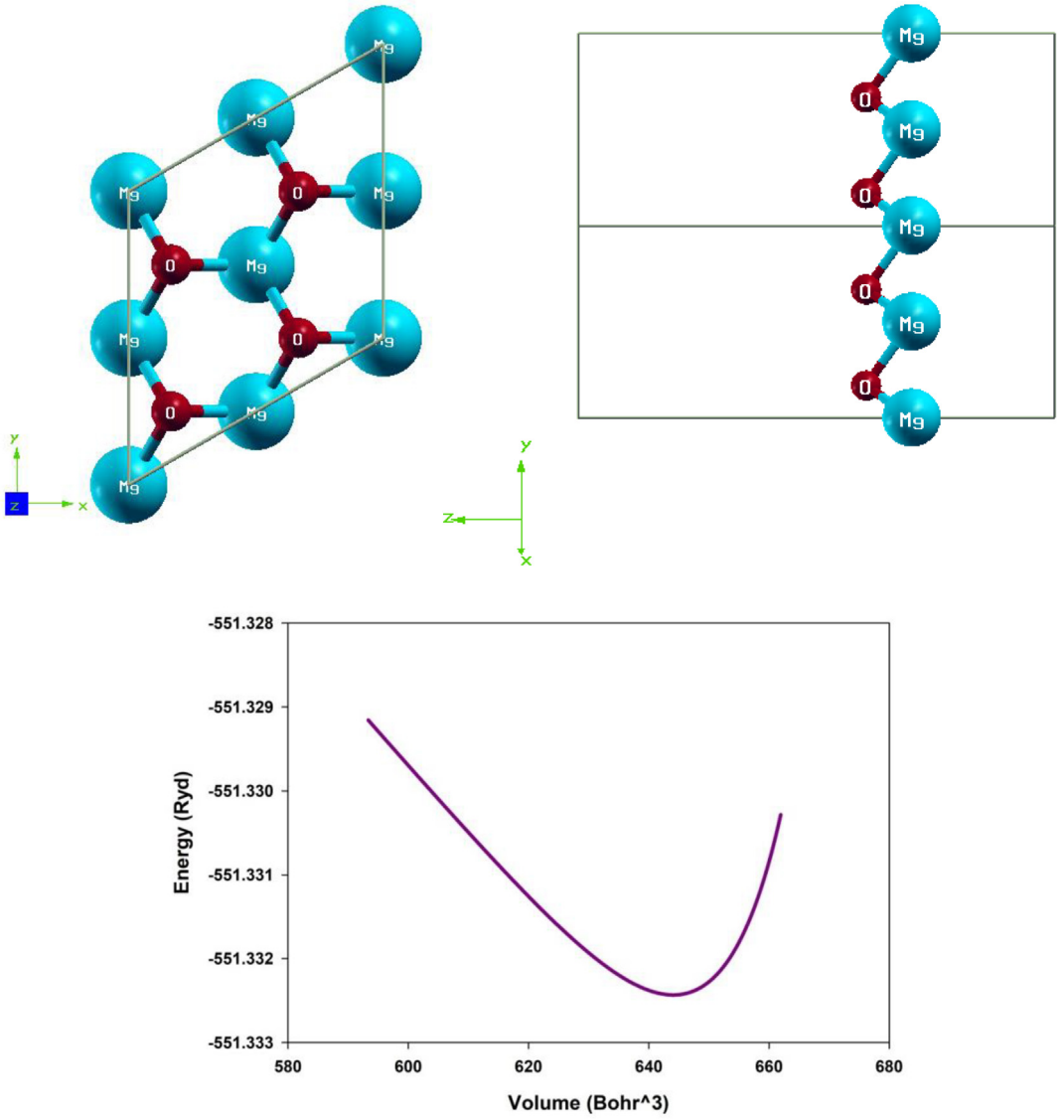

Fig. 1. The MgO-monolayer structure of the top and side views and energy-volume (E-V) diagram.

Computational methods

The calculations were done using DFT with full potential linear augmented plane waves plus local orbital (FP-LAPW + lo) methods by GGA approximations in the Wien2K code [30–32]. The input parameters such as RKmax, KPoint and Gmax are optimized to 8.0, 5000 and 13.0, respectively. Also, to achieve the optimum atomic positions, the atomic positions of the crystal lattice were relaxed to 1.0 mRyd/a.u., also the crystal volume versus energy was optimized based on the Brich-Mornaghan equation at Fig. 1. Moreover, for increasing calculations accuracy, the accuracy of electron charge density is selected to 0.00001 (e/bohr^3) and the optical calculations have been performed by random phase approximation (RPA) [33]. The crystal lattices of the MgO mono-layer in the two views are depicted in Fig. 1 which is made of the MgO bulk structure by cutting it along the [1 1 1] direction with the Octave software. Fig. 1 has been shown that the MgO-monolayer has the mechanical stability by an equilibrium volume. For more investigation about MgO mono-layer stability in the energy view, the cohesive energy by GGA and mBJ approximations were calculated and found to be −5.89 eV and −5.34 eV, respectively, indicating good stability for this case.

Results

Electronic properties

The electronic density of states (DOS) curve is one of the useful tools to specify the electronic and even optical behavioral features of matter. The DOS of MgO mono-layer by GGA and GGA-mBJ approximations are depicted in Fig. 2, which the Mg atom with atomic number 12 by $3s^2$ valance orbital participating Oxygen with atomic number 8 ending with $2p^4$ make strong covalent bonds (sp^2) in the plane of MgO- (G-L). As shown in Fig. 2, the combination of Mg (metal) and O creates a perfect semiconductor, so that the semiconducting behavior is well observed in both approximations. The obtained energy gaps for bulk phase by both mentioned approximations are listed in Table 1, indicating that the mBJ amount is in good agreement with other's (ref [14]) which prove the accuracy of our calculations.

Both approximations emphasize on the p-type semiconducting property of MgO mono-layer, but the mBJ approximation has resulted a shift in the valance band maximum (VBM) to the lower energies so its energy gap is greater than GGA one. The teeth-saws form of the DOS diagram implies its nano-size and the continually of states in the conduction region indicates that this material is a good electron transporter

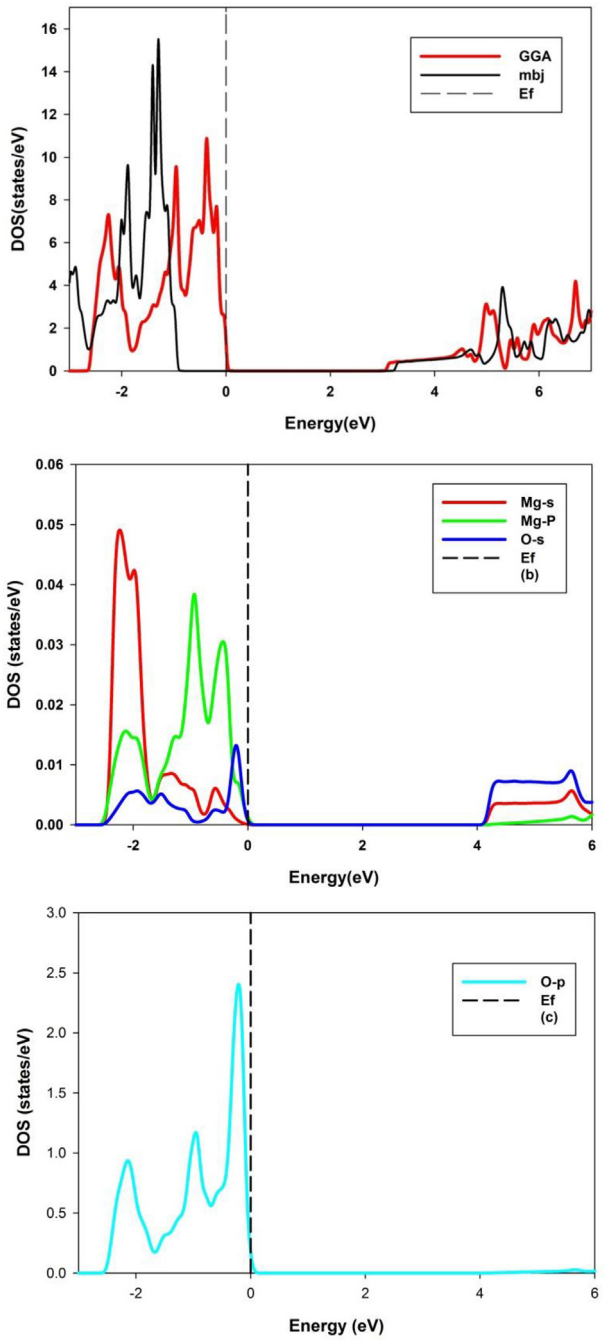

Fig. 2. The total DOS of MgO mono-layer: (a) GGA-mBJ, GGA (b & c) The Partial DOS with mBJ.

Table 1
The obtained gaps for both approximations in G-L and bulk states.

	Bulk-(GGA)	Bulk-(mBJ)	MgO-(G-L) (GGA)	MgO-(G-L) (GGA-mBJ)
Gap (eV)	4.835	7.286 7.8 eV[a]	3.1 eV	4.2 eV

[a] [14].

in the electronic or optical view. From the edge of the gap until some higher energy, the electronic states are continually increased with increasing the energy of levels, which is a positive point for conduction of electrons being able to jump from the valence to the conduction band. A remarkable point is that the bulk structure of MgO is a perfect insulator with a high amount of gap. But in MgO mono-layer, the electrostatic potential is increased on the surface of this nanosheet due to the presence of π electrons, so the conduction electronic states belonging to p orbital to the Fermi level result a sensible decrement of the energy gap of this structure. These features make MgO a promising compound for optical and optoelectronic use and even solar cells.

Fig. 3 depicts the band structure curve of MgO nanosheet on symmetric directions in the first Brillouin zone which indicates the direct gap at Γ point by GGA and mBJ. An implicit point is that the energy levels in the valence band have a very low curve slope, resulting very low group velocity and very high effective mass of electrons. The electrons are hard and heavy particularly in the Fermi level, so that in the Γ-X region, the effective electron mass is almost very large and the corresponding group velocity is zero. This result implies that the *s* orbital of Oxygen and *p* of Magnesium have made a sp^2 bond with strong covalent bonds. But the electron levels in the conduction bands, especially in the CMB, have great gradient along the Γ symmetry point and the Γ-X and M-Γ paths; so that there is a very low effective mass and high group velocity for electron. Thus, when an electron is pumped to this area, it is well streamed in the conduction current, and this is a very promising point for this nanosheet. In general, from the diagrams of the electronic part, we find that MgO-(G-L) is a very promising and good compound for electronics industry, so that the strong bonds make its structure and gap more stable, and also its low effective mass and good conductivity lead to a good performance in optoelectronics industry.

Optical properties

The dielectric function (ε(ω)) is the material's response to incident light consisting of two real and imaginary parts, which forms a 3 × 3 tensor. Our calculations are based on the RPA approximation, and the calculated ε(ω) is the same as the main tensor diagonal elements, so that $\varepsilon_{xx} = \varepsilon_{yy} \neq \varepsilon_{zz}$. Fig. 4 shows the real part of dielectric function (Re-ε(ω)) curve on two directions x and z (in the planes of MgO-(G-L) and one perpendicular to it) by GGA and mBJ approximations. The static value of Re-ε(ω) in both directions is about 1.5 indicating the strong semiconducting behavior of this compound in both directions by GGA calculation and is about 1.4 for mBJ one, which claims a greater energy gap in this approximation. However, the GGA calculation indicates that by increasing the energy of the incident photon to about 4 eV (the energy gap area of the matter), Re-ε(ω) remains relatively constant and will not change too much; this happens because no electron has been able to traverse the band gap of this compound yet. Thereafter, with increasing the photon energy, the response to the incident light in both directions increases with a rather steep slope, so that peaks are appeared in the range about 7 eV, and by changing the direction of the incident light, the response along z axis is a blue shift.

However, the amplitude of response to incident light decreases by increasing photon energy in both directions reaching its minimum at energy of 20 eV, and the semiconductor-like and even insulator behavior is observed. So that, in the range of 10 eV, the value of Re-ε(ω) in both directions is less than 1. Another point is that the anisotropic behavior for both of these directions is observed after 5 eV range. The mBJ calculation is similar to the GGA one with a blue shift of the Re-ε(ω) peaks in the 4 eV to 9 eV range. It is shown that the main difference between two mentioned approximations is occurred in the lower photon energies.

Imaginary part of ε(ω) (Im-ε(ω)) contains very important information about band structure and materials' energy. So that, one may specify energy gap from Im-ε(ω) diagram and detect electron transitions from occupied to unoccupied levels from its peaks which is indicated in Fig. 5.

As shown in Fig. 5, from zero energy to 4.1 eV, a gap is observed which is the same MgO mono-layer electronic gaps in the mBJ calculations, the amount of this gap is independent of the direction of the incident light. However, after the range of 4.1 eV, a very strong increase

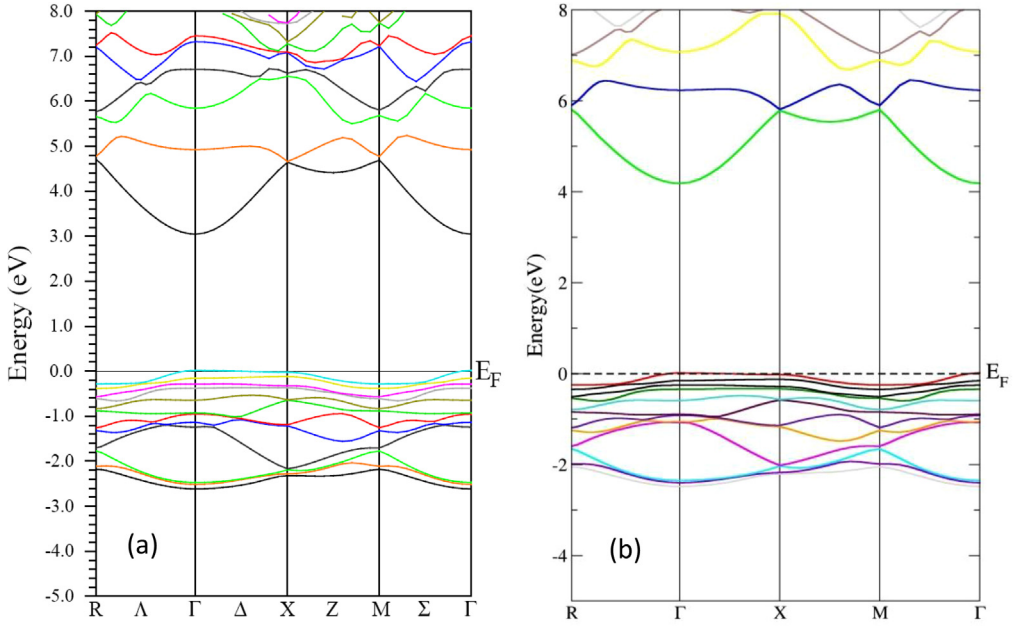

Fig. 3. The band structure curve of MgO nanosheet on symmetric directions of the first Brillouin zone (a) GGA, (b) mBJ.

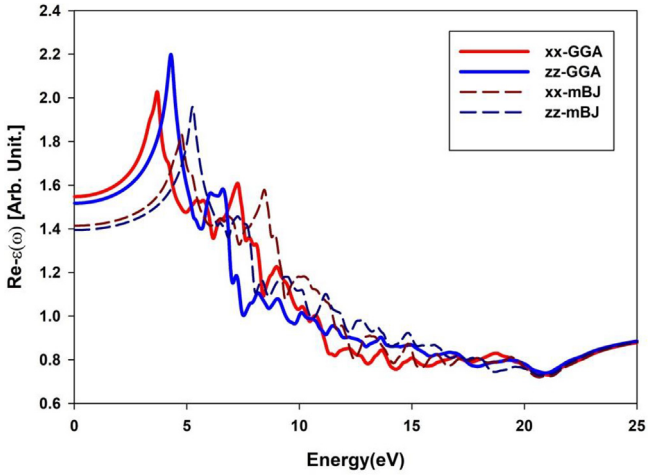

Fig. 4. The Re-ε(ω) versus photon energy of MgO mono-layer at two *x* and *z* directions by GGA and mBJ.

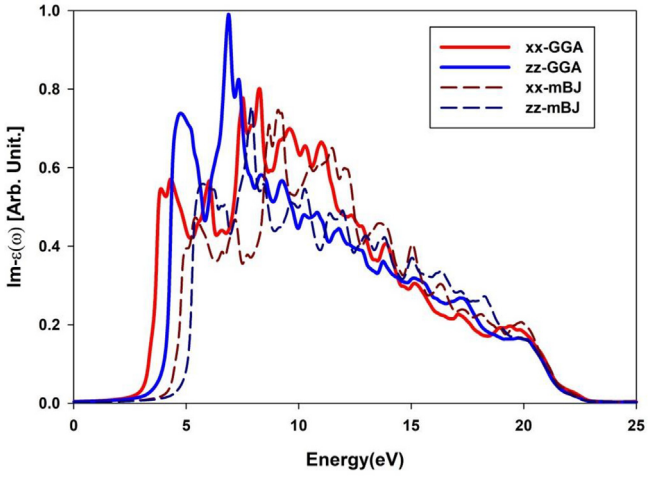

Fig. 5. The Im-ε(ω) of MgO mono-layer of two *x* and *z* directions with GGA and mBJ approximations.

in the Im-ε(ω) curves is observed, where 5 eV peaks indicate the first transition from the valence to the conduction band of this compound. As the incident photons intensity increases, the amount of transitions is gradually reduced. Most of these transitions occur from the orbitals 3s and 2p of Mg to the orbital 2p of Oxygen. After 23 eV no transitions occurred and this case is similar to the transparent matters. After 10 eV the mBJ results is similar to the GGA with some differences, such as decreasing the peaks numbers, the blue shift of the Im-ε(ω) peaks and increase in the Im-ε(ω) gap.

The Eloss diagram in Fig. 6 by the GGA calculation shows that there is no graph in the gap region as expected. But naturally, after the gap region as the matter reaction to the incident light begins, a part of this light is lost which is shown in the figure, and its Eloss gap is greater for mBJ one, which is in agreement with electronic gap.

At the UV edge, most of the amount of loss function (Loss) is occurred along the z axis. But the maximum Loss values is occurred in the range of 10–15 (eV), which is related to the direction of the x axis, and also, we see severe anisotropy in this area by two approximations. The Eloss of incident light might be due to several reasons including plasmonic fluctuations, which, of course, has not happened in this

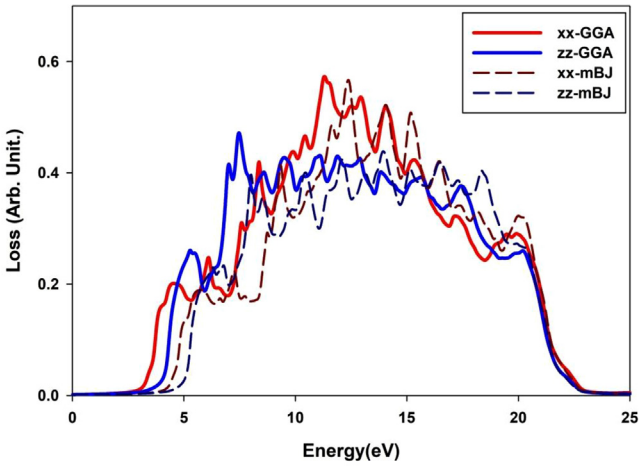

Fig. 6. The energy loss function of MgO mono-layer versus photon energy for *x* and *z* directions by GGA and mBJ.

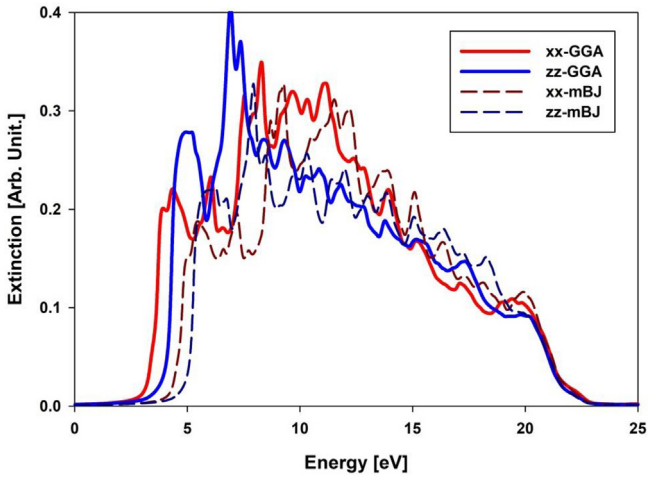

Fig. 7. The extinction coefficient of MgO mono-layer for *x* and *z* directions by GGA and mBJ.

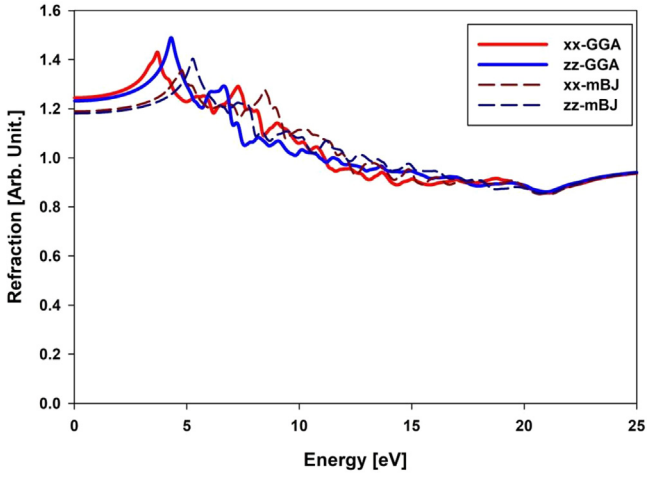

Fig. 8. The refraction coefficient of the MgO mono-layer in the two *x* and *z* directions by GGA and mBJ.

structure. Another reason for loss might be due to the amount of extinction coefficient of the material, and by comparing the ELoss function with the extinction coefficient curve in Fig. 7, it is observed that the maximum of the extinction coefficient take place in the same range.

The refraction index curve of this compound for the two mentioned directions is shown in Fig. 8. The static refraction index is quite uniform for both directions up to the edge of the energy gap, and is equal to 1.24 in GGA but are smaller for mBJ one, indicating a great semiconducting behavior. But in the range 5–6 eV, where the electron transition occurs and Re-ε(ω) is peaked, there is a relative increase in the refraction index, but with increasing energy of the incident photon, the refraction index amplitude decreases slowly so that after 10 eV, the refraction index in both directions is less than one, in which case the MgO mono-layer plays the role of an accelerator for the light, and the speed of light in the material exceeds the speed of light in the vacuum representing the superluminal phenomenon for the two mentioned approximations.

The imaginary part of refraction coefficient defines the extinction coefficient, which refers to the reduction amount in the amplitude of light in the material. As shown in Figs. 4 and 7, the matter's response to the incident light in the Re-ε(ω) curve is occurred in the range of 5 eV. By increasing the light energy, the amount of this response is decreased as a result of the behavior of the extinction coefficient curve, since the most amounts of light loss occurs in this region. Of course, the numeric value of the extinction coefficient of this compound is not that large

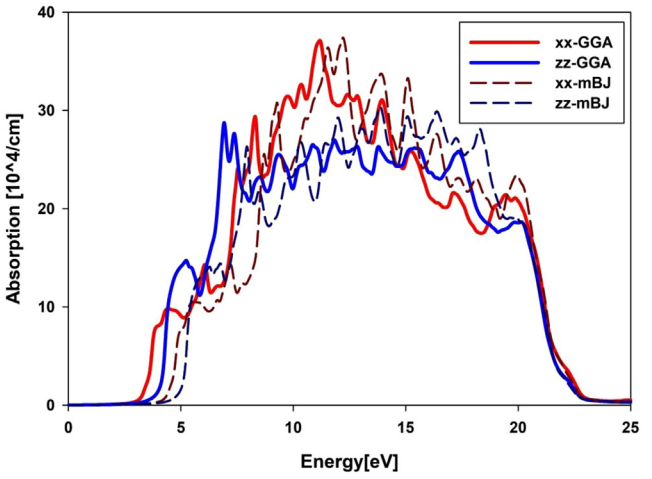

Fig. 9. The Absorption index of MgO mono-layer versus photon energy by GGA and mBJ.

compared to other compounds. The starting points of the extinction coefficients are first occurred for GGA and then for mBJ.

Finally, the refraction coefficient curve of MgO mono-layer is shown in Fig. 8 for x and z directions of the two calculation modes. The very low static extinction coefficient indicates that this compound is essentially opaque. Also, the highest magnitude of MgO mono-layer refraction coefficient in both directions is between 0.025 and 0.30, which is very small, refracting maximally three percent of the light while leaving the remaining absorbed or transited. Comparing the absorption curve in Fig. 9 and Im-ε(ω) in Fig. 5, it is observed that most of the absorbed light passes through the material or is used up on the electron transitions. Therefore, in this range of energy (10–20 eV), unlike the low energies, this is a transparent material, while it is opaque at low energies, which shows that varying the energy of incident photons leads to different optical behaviors in this compound. It is shown that GGA results a red shift in the absorption, and at the UV area the absorption treatment of the two approximations are the same.

Conclusion

Base on the DFT calculations with FP-LAPW + lo method and using GGA and mBJ approximations, the electronic, optical properties of MgO-monolayer where calculated. The electronic results including the DOS and band structure diagrams indicated the semiconducting behavior by a direct gap at Γ symmetry point for 3.1 eV and 4.2 eV using GGA and mBJ respectively. The electronic results are also indicated good semiconducting behaviors as high electron mobility were observed at conduction band.

The statics amount of Re-ε(ω) confirmed the semiconducting behavior of MgO Mono-layer and its amount accrued at the edge of UV. The Im-ε(ω) for two x and z directions showed an energy gap in agreement with the electronic gap. Also, the Eloss of photon energy, absorption and extinction coefficient amounts are in the high photon energy range (10–20 eV), suggesting that the MgO mono-layer is a good candidate for applications in the UV area. The optical results indicated a blue shift in mBJ calculations which was not observed in GGA one.

References

[1] Jeanloz R, Ahrens TJ. Geophys J R Astron Soc 1980;62:505.
[2] Chang KJ, Cohen Marvin L. Phys Rev B 1984;30:4774.
[3] Singh Jitendra Pal, Ji Mi-Jung, Kumar Manish, Lee Ik-Jae, Chae Keun Hwa. J Alloy Compd 2018;748:355.
[4] Barman Sukanta, Kundu Asish K, Menon Krishnakumar SR. Surf Sci 2018;677:60.
[5] Stachowicz M, Pietrzyk M, Jarosz D, Dluzewski P, Kozanecki A. Surf Coat Technol 2018;355:45.
[6] Duffy TS, Hemley RJ, Mao H-K. Phys Rev Lett 1995;74:1371–4.

[7] Park WI, Yi G-C, Jang HM. Metalorganic. Appl Phys Lett 2001;79:2022–4.
[8] Xu L-C, Wang RZ, Miao M, Wei, et al. Nanoscale 2014;6:1113.
[9] Cahangirov S, Topsakal M, Akturk E, Sahin H, Ciraci S. Phys Rev Lett 2009;102:236804.
[10] Zhou XF, Dong X, Oganov AR, Zhu Q, Tian YJ, Wang HT. Phys Rev Lett 2014;112:085502.
[11] Zhang LZ, Wang ZF, Du SX, Gao HJ, Liu F. Phys Rev B: Condens Matter Mater Phys 2014;90:161402.
[12] Arash Boochani, Bromand Nowrozi, Jabbar Khodadadi, Shahram Solaymani, Saeid Jalali-Asadabadi. 121(2017):3978.
[13] Bromand Nourozi, Arash Boochani1 Ahmad Abdolmaleki, Elmira Sartpi, PezhmanDarabi, SirvanNaderi. 69(2018):101.
[14] Song Zhenjun, Zhao Bin, Wang Qiang, Cheng Peng. Appl Surf Sci 2018;459:812.
[15] Singh Jitendra Pal, Lim Weon Cheol, Lee Jihye, Song Jonghan, Chae Keun Hwa. Appl Surf Sci 2018;432:132.
[16] Roessler DM, Walker WC. Phys Rev 1967;159:733.
[17] Fiermans L, Hoogewijs R, de Meyer G, Vennik J. Phys Status Solidi A 1980;59:569.
[18] El-Sayed Al-Moatasem, Watkins Matthew B, Grasser Tibor, Shluger Alexander L. Phys Rev B 2018;98:064102.
[19] Abdul-MuizzPradipto Toru Akiyama, Ito Tomonori, Nakamura Kohji. Phys Rev B 2018;97:024401.
[20] Fernandes Edgar, Donati Fabio, Patthey François, Stavrić Srdjan, Šljivančanin Željko, Brune Harald. Phys Rev B 2017;96:045419.
[21] Pong CY, Saslow, Cohen ML. Phys Rev 1968;168:992.
[22] Raju S, Sivasubramanian K, Mohandas E. Physica B 2002;324:312.
[23] Wang Deyong, Li Xiaobing, Wang Huihua, et al. J Non-Cryst Solids 2012;358:1196.
[24] Bukowinski MST. J Geophys Res 1980;85:285.
[25] Yamashita J, Asano S. J Phys Soc Jpn 1970;28:1143.
[26] Yu BD, Kim J-S. Phys Rev B 2006;73:125408.
[27] Meyerheim HL, Popescu R, Jedrecy N, Vedpathak M, Sauvage-Simkin M, Pinchaux R, et al. Phys Rev B 2002;65:144433.
[28] Delle Site L, Alavi A, Lynden-Bell RM. J Chem Phys 2000;113:3344.
[29] Rasmussen Filip A, Thygesen Kristian S. J. Phys Chem C 2015;119:13169–83.
[30] Blaha P, Schwarz K, Sorantin P, Tricky SB. Com-put Phys Commun 1990;59:399.
[31] Blaha P, Schwarz K, Madesen GKH, et al. WIEN2K an Augmented Plane Wave Local OrbitalsProgram for Calculating Crystal Properties. Wien, Austria: KarlheinzSchwarz, Techn. Universitaetwien; 2001.
[32] Perdew J, Chevary JA, Vosko SH, et al. Phys Rev B 1992;46:6671.
[33] Kronig RL. J Opt Soc Am 1926;12:547.